Impacts of hexadecapole deformations on the collective energy spectra of axially deformed nuclei

L. Lotina [1,*] and K. Nomura [2,3,†]

[1]*Department of Physics, Faculty of Science, University of Zagreb, HR-10000 Zagreb, Croatia*

[2]*Department of Physics, Hokkaido University, Sapporo 060-0810, Japan*

[3]*Nuclear Reaction Data Center, Hokkaido University, Sapporo 060-0810, Japan*

(Received 11 October 2023; accepted 8 February 2024; published 5 March 2024)

The hexadecapole deformation, as well as the quadrupole one, influences the low-lying states of finite nuclei. The hexadecapole correlations are often overshadowed by the large quadrupole effects, and hence have not been much investigated. Here we address the relevance of hexadecapole deformations in the calculations of low-energy collective states of heavy nuclei, by using the theoretical framework of the self-consistent mean-field method and the interacting-boson approximation. The interacting-boson Hamiltonian that explicitly includes the quadrupole and hexadecapole collective degrees of freedom is specified by a choice of the energy density functional and pairing interaction. In an illustrative application to axially deformed Gd isotopes, it is shown that the inclusion of the hexadecapole degree of freedom does not affect most of the low-spin and low-lying states qualitatively, but that has notable effects in that it significantly improves the description of high-spin states of the ground-state bands of nearly spherical vibrational nuclei and gives rise to $K^\pi = 4^+$ bands exhibiting strong $E4$ transitions in strongly deformed nuclei.

DOI: 10.1103/PhysRevC.109.034304

I. INTRODUCTION

Deformation of the nuclear surface and the corresponding collective excitations are a prominent aspect of the atomic nucleus [1]. Among those collective excitation modes that correspond to positive-parity states of nuclei, the dominant and most studied is of quadrupole type, while much less attention has been paid to the next leading order, hexadecapole deformation. This is mostly because the effects of the hexadecapole correlations in nuclear low-lying states are often overshadowed by large quadrupole correlation effects. The hexadecapole correlations, nevertheless, have been shown to be present in many rare-earth [1–5], and actinide [6,7] nuclei, as well as some light ones [8], and have recently been found in exotic isotopes with an unusual proton to neutron number ratio [9]. Notable hexadecapole effects in nuclear collective structure include the appearance of the low-energy $K^\pi = 4^+$ bands and enhanced electric hexadecapole ($E4$) transitions. Furthermore, recent hydrodynamic simulation has indicated that the hexadecapole deformation plays a role in modeling heavy ion collisions studied at the Relativistic Heavy Ion Collider [10]. In addition, various nuclear deformation effects, including that of hexadecapole type, should have influences on the predictions of the neutrinoless double decay matrix elements of open shell nuclei [11].

It is, therefore, interesting and timely to study impacts of hexadecapole deformations on nuclear structure in a quantitative and systematic way, using a model that allows for an accurate description of excitation spectra and electromagnetic transition properties of low-lying collective states. Among other nuclear structure models, the interacting boson model (IBM) [12] has been successful for phenomenological descriptions of low-energy collective excitations in medium-heavy and heavy nuclei. The basic assumption of the IBM is that the nuclear low-lying states are described in terms of s and d bosons, which reflect [13] the collective monopole, S (with spin 0^+), and quadrupole, D (spin 2^+), pairs of valence nucleons, respectively. The IBM should have certain microscopic foundations on the underlying nucleonic dynamics, and attempts have been made to derive the model Hamiltonian from more microscopic nuclear structure calculations [13–16]. In particular, a mapping technique has been developed [15] that links the IBM to the framework of the nuclear energy density functional (EDF). This procedure has been successfully applied to describe quadrupole [15–18] and octupole [19,20] collective states.

In addition to s and d bosons, spin 4^+, or g, bosons have often been considered in the IBM [12]. The importance of g bosons in describing spectroscopic properties of deformed nuclei has been addressed from various perspectives [21–31]. Some of these earlier studies also concern the validity of the sd-IBM from a microscopic point of view, that is, the question as to whether the g boson degrees of freedom are indispensable or not for a precise description of axially deformed nuclei [21–24,26]. Along with the strongly deformed regions, it should be also of interest to investigate the significance of the hexadecapole correlation effects in those nuclei in nearly spherical vibrational and transitional regions.

In this article, we implement the hexadecapole (g boson) degree freedom in the IBM by means of the aforementioned

*llotina.phy@pmf.hr

†nomura@sci.hokudai.ac.jp

mapping procedure [15], and demonstrate that the hexadecapole effects are present in the low-energy collective states of heavy nuclei in the nearly spherical vibrational region as well as in the strongly deformed region. As an illustrative example we focus on the isotopic chain of axially deformed $^{148–160}$Gd nuclei, which exhibits a manifest first-order shape phase transition from spherical to (quadrupole) deformed shapes [32], and for which hexadecapole collectivity has also been suggested to emerge empirically.

II. SCMF ENERGY SURFACES AND MAPPING ONTO THE IBM

Our analysis begins with the self-consistent mean-field (SCMF) calculations using a nuclear EDF. The nuclear EDF approaches are nowadays among the most reliable theoretical methods of studying intrinsic and excited states of finite nuclei [33–40], and hexadecapole deformations have also been considered as additional collective coordinates (see, e.g., Refs. [10,41,42]). For the $^{148–160}$Gd isotopes, we perform the SCMF calculations within the multidimensionally constrained relativistic mean-field (MDC-RMF) model [40,43] and obtain energy surfaces in terms of the axial quadrupole (β_2) and hexadecapole (β_4) deformations, which are shown on the left column of Fig. 1. The SCMF calculations are here carried out within the relativistic Hartree-Bogoliubov framework [36,38] using the density-dependent point-coupling (DD-PC1) interaction [44] and the separable pairing force of finite range [45]. The constraints are on the expectation values of axial quadrupole $\hat{Q}_{20}$ and hexadecapole $\hat{Q}_{40}$ moments, which are related to the deformation parameters β_2 and β_4 through the relation, $\beta_\lambda = (4\pi/3AR^\lambda)\langle\hat{Q}_{\lambda 0}\rangle$ with $\lambda = 2, 4$ and $R = 1.2A^{1/3}$ fm.

As one can see in Fig. 1, for most of the Gd nuclei, the hexadecapole deformed ground state with a positive β_4 value is obtained in the SCMF energy surfaces: the global minimum occurs at the deformations $(\beta_2{}^{\rm min}, \beta_4{}^{\rm min}) \approx (-0.05, 0)$, $(0.15, 0.05)$, $(0.2, 0.1)$, $(0.3, 0.15)$, $(0.3, 0.15)$, $(0.35, 0.15)$, and $(0.35, 0.15)$ for $^{148–160}$Gd, respectively. Both the $\beta_2{}^{\rm min}$ and $\beta_4{}^{\rm min}$ values keep increasing with the neutron number, but the latter changes more slowly than the former. One notices that there is no $\beta_4 \neq 0$ minimum on the energy surface of ^{148}Gd. The potential is nevertheless rather soft along the β_4 direction, softest among the considered Gd isotopes. The softness in β_4 implies that the hexadecapole correlations play an important role in this nucleus, and, as we show below, to account for the β_4 softness the g boson degree of freedom is required. These findings, regarding the β_2-β_4 energy surfaces, are consistent with earlier SCMF results obtained for the same mass region, e.g., the one with the axially deformed Woods-Saxon potential involving the hexadecapole degree of freedom [46], and a more recent beyond-SCMF calculation that is based on the Gogny forces dealing with the quadrupole-hexadecapole coupling [42].

The SCMF results are then used to construct the Hamiltonian of the s, d, and g boson system (denoted as sdg-IBM), which gives rise to excitation energies and electromagnetic transition rates. For the sdg-IBM Hamiltonian, we exploit the form that has been been shown to be adequate for

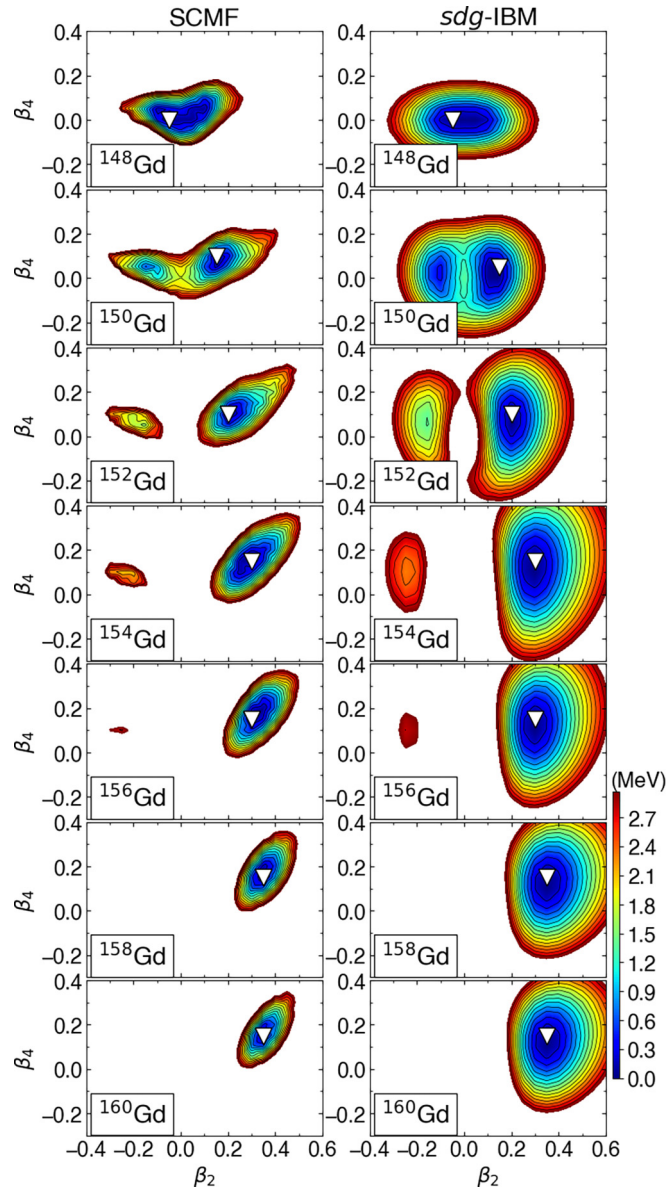

FIG. 1. Left column: axially symmetric quadrupole (β_2) and hexadecapole (β_4) constrained energy surfaces for the $^{148–160}$Gd isotopes calculated within the relativistic Hartree-Bogoliubov method using the density-dependent point-coupling energy density functional and the pairing force of finite range. Right column: the corresponding energy surfaces of the sdg-IBM. The global minimum is indicated by the open triangles.

phenomenological descriptions of shape phase transitions with quadrupole and hexadecapole degrees of freedom [31]:

$$\hat{H}_{\rm sdg} = \epsilon_d \hat{n}_d + \epsilon_g \hat{n}_g + \kappa \hat{Q}\cdot\hat{Q} + \kappa(1-\chi^2)\hat{Q}'\cdot\hat{Q}', \qquad (1)$$

where the first and second terms in the right-hand side stand for the d-, and g-boson number operators, $\hat{n}_d = d^\dagger\cdot\tilde{d}$ and $\hat{n}_g = g^\dagger\cdot\tilde{g}$, respectively. The third term represents the quadrupole-quadrupole interaction. The quadrupole operator,

$\hat{Q}$, takes the form

$$\hat{Q} = s^\dagger \tilde{d} + d^\dagger s + \chi \left[\frac{11\sqrt{10}}{28} (d^\dagger \times \tilde{d})^{(2)} - \frac{9}{7} (d^\dagger \times \tilde{g} + g^\dagger \times \tilde{d})^{(2)} + \frac{3\sqrt{55}}{14} (g^\dagger \times \tilde{g})^{(2)} \right], \quad (2)$$

which is the expression considered also in Ref. [31] and corresponds to a generator of sdg-SU(3) in the limit $\chi = 1$ [31,47]. The last term on the right-hand side of Eq. (1) represents the hexadecapole-hexadecapole interaction, with the hexadecapole operator being $\hat{Q}' = s^\dagger \tilde{g} + g^\dagger s$. In principle, the hexadecapole operator in the sdg-IBM could take a more complicated form that contains some other terms. The reason why we end up with the simplified form that comprises the $s^\dagger \tilde{g} + g^\dagger s$ terms only is because the SO(15) symmetry is assumed on the sdg-IBM Hamiltonian (see Refs. [28,31] for the details). In addition, for the sake of simplicity no distinction is made between the neutron and proton degrees of freedom. While a more realistic study would require that neutron and proton bosons be treated separately, it is expected that there is no qualitative difference in the description of the low-lying yrast states of most of the medium-heavy and heavy nuclei between the IBM that comprises neutron and proton bosons and the one in which they are not distinguished. The distinction between neutron and proton bosons would be relevant when describing phenomena such as the neutron-proton mixed symmetry states and the related magnetic dipole properties, in which the neutron and proton degrees of freedom play an important role. On the other hand, the scope of present work is to study the effect of g bosons on energy spectra, and for the initial application of the mapped sdg-IBM framework to realistic cases, it would be sufficient to use a simpler version of the sdg-IBM, where the neutrons and protons are not distinguished.

The parameters of the Hamiltonian (1) (ϵ_d, ϵ_g, κ, and χ) are determined, for each nucleus, by applying the method of Ref. [15]: the β_2-β_4 SCMF energy surface, $E_{\rm SCMF}(\beta_2, \beta_4)$, is mapped onto the equivalent energy surface of the boson system, $E_{\rm IBM}(\tilde{\beta}_2, \tilde{\beta}_4)$, so that the approximate equality,

$$E_{\rm SCMF}(\beta_2, \beta_4) \approx E_{\rm IBM}(\tilde{\beta}_2, \tilde{\beta}_4), \quad (3)$$

should be satisfied in the neighborhood of the global minimum. Here, $E_{\rm IBM}(\tilde{\beta}_2, \tilde{\beta}_4)$ is given as the expectation value of the Hamiltonian (1) in the coherent state $|\phi\rangle$, with $|\phi\rangle \propto (1 + \tilde{\beta}_2 d_0^\dagger + \tilde{\beta}_4 g_0^\dagger)^{N_{\rm B}} |0\rangle$ [28,48]. $N_{\rm B}$ stands for the number of bosons, which is equal to half the number of valence nucleons, and the ket $|0\rangle$ represents the inert core, i.e., the doubly magic nucleus ^{132}Sn. The amplitudes $\tilde{\beta}_2$ and $\tilde{\beta}_4$ stand for the boson analogs of the axial quadrupole and hexadecapole deformations, respectively, and are assumed to be proportional to the fermionic counterparts, that is, $\tilde{\beta}_2 \propto \beta_2$ and $\tilde{\beta}_4 \propto \beta_4$. See Refs. [15,16] for further details of this mapping procedure in the case of *sd*-IBM.

On the right column of Fig. 1, we show the mapped sdg-IBM β_2-β_4 deformation energy surfaces. One can see that the basic characteristics of the SCMF energy surface, such as the depth of the potential and the coordinates corresponding to the global minimum [$(\beta_2^{\rm min}, \beta_4^{\rm min})$], are reproduced in the mapped sdg-IBM surfaces.

To compare with the sdg-IBM results, we also carry out the calculations within the original version of the IBM, that comprises s and d bosons only (*sd*-IBM). The *sd*-IBM Hamiltonian here takes the standard form [12]

$$\hat{H}_{sd} = \epsilon_d \hat{n}_d + \kappa \hat{Q}_{sd} \cdot \hat{Q}_{sd}, \quad (4)$$

where $\hat{Q}_{sd} = s^\dagger \tilde{d} + d^\dagger s + \chi_d (d^\dagger \times \tilde{d})^{(2)}$ is the quadrupole operator for the (s, d)-boson systems. The three parameters, ϵ_d, κ, and χ_d, are determined by mapping the SCMF energy surface along the β_2 deformation with $\beta_4 = 0$ onto that of the *sd*-IBM, that is, $E_{\rm SCMF}(\beta_2, \beta_4 = 0) \approx E^{sd}_{\rm IBM}(\tilde{\beta}_2)$.

III. RESULTS

Figures 2(a) and 2(b) show the excitation energies of even-spin positive-parity states in the ground-state bands of $^{148–160}$Gd, obtained from the diagonalization [50] of the mapped *sd*- and sdg-IBM Hamiltonians, respectively, compared to the corresponding experimental data [49]. A noticeable influence of including the hexadecapole deformation on the ground-state bands is that the excitation energies of the states with spin $I^\pi \geqslant 6^+$ calculated within the sdg-IBM for those nuclei with $N = 84$ and 86, which are close to the neutron magic number $N = 82$, are much lower than in the *sd*-IBM, and are in agreement with experiment.

The calculated ratios of the first 4^+ to 2^+ excitation energies, $R_{4/2} = E_x(4_1^+)/E_x(2_1^+)$, obtained from the sdg (*sd*) IBM are,1.86 (2.13), 2.15 (2.18), 2.38 (2.36), 2.84 (2.83), 2.99 (3.08), 3.10 (3.24), 3.16 (3.23) for $^{148–160}$Gd, respectively. The observed $R_{4/2}$ ratios, on the other hand, are equal to 1.81, 2.02, 2.19, 3.02, 3.24, 3.26, and 3.32 for $^{148–160}$Gd, respectively [49]. By comparing the theoretical and experimental $R_{4/2}$ ratios, it turns out that another significant impact of g bosons is that the sdg-IBM reproduces the experimental $R_{4/2}$ ratio for the ^{148}Gd nucleus, $R_{4/2} = 1.81 < 2$. The experimental value of $R_{4/2} < 2$ could be reproduced only by the inclusion of g bosons, since it lowers the 4_1^+ level to be close in energy to the 2_1^+ one. The fact that the observed $R_{4/2}$ ratio for ^{148}Gd is lower than two also reflects, to a good extent, the contribution from the single-particle excitations, which appear to be effectively accounted for by the inclusion of g bosons.

Even though g bosons, as well as s and d bosons, are considered as collective in nature, the fact that the inclusion of g bosons in the IBM significantly improves description of the observed energy ratio of $R_{4/2} < 2$, as well as the fact that the ground-state yrast levels with $I \geqslant 6$ is reproduced quite well, indicates that g bosons are considered as necessary building blocks to describe the low-energy excitations in the nuclei with $N = 84$ and 86, where single-particle degrees of freedom come to play a role. We also note that both the *sd*-IBM and sdg-IBM have often been applied to nearly spherical and moderately deformed nuclei with N being near shell closure, and has been shown to be valid in a number of phenomenological applications and in the microscopic considerations.

The lowering of the higher spin levels of the ground-state bands for the nearly spherical nuclei is explained by the increasing g boson contribution to the wave functions as a

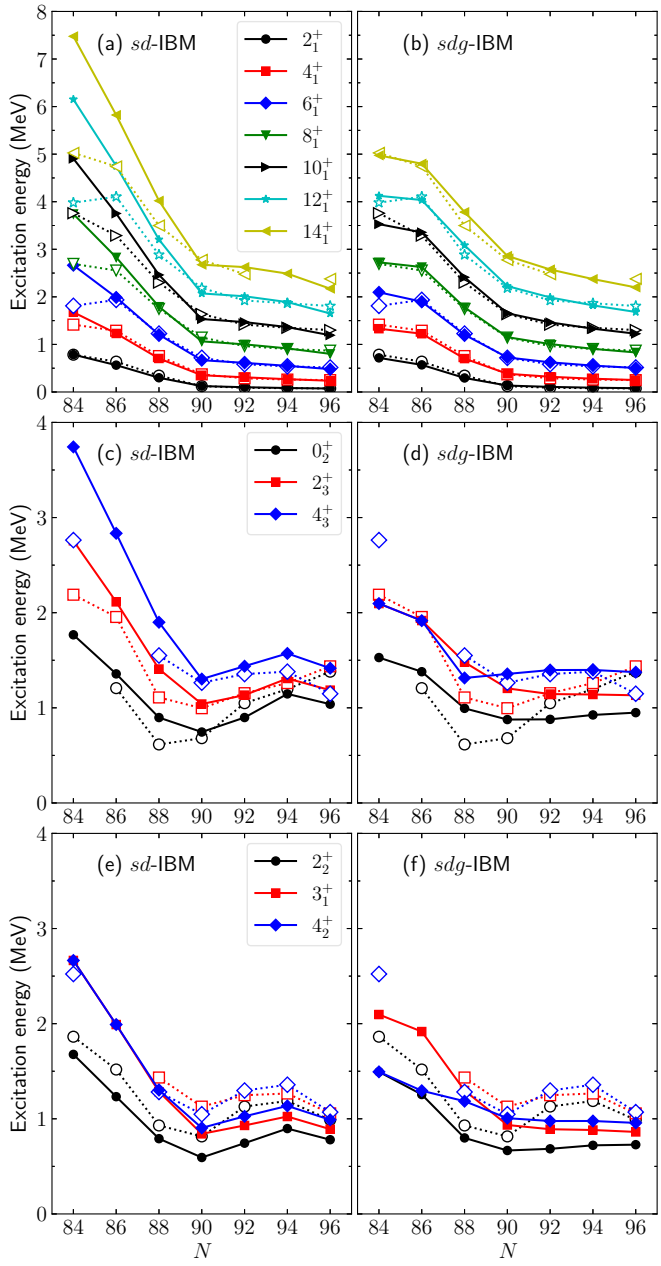

FIG. 2. Energy spectra of positive-parity even-spin yrast states [panels (a) and (b)], 0_2^+, 2_3^+, and 4_3^+ states [panels (c) and (d)], and 2_2^+, 3_1^+, and 4_2^+ states [panels (e) and (f)] of $^{148-160}$Gd calculated with the *sd*- (left column), and sdg-IBM (right column) in comparison with the experimental data [49]. The calculated excitation energies are represented by filled symbols, and the corresponding experimental data by the open symbols.

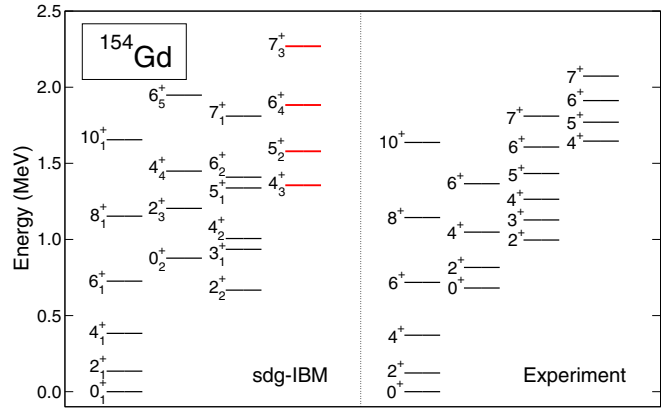

FIG. 3. Low-spin part of the positive-parity bands of ^{154}Gd calculated with the sdg-IBM, in comparison with the experimental data [49]. The theoretical band that is built on the 4_3^+ state, highlighted in thick lines with color red, is predicted to be of one-*g*-boson character.

function of spin. The contribution of g bosons to a given state is inferred from the expectation value, $\langle \hat{n}_g \rangle$, computed by using the sdg-IBM wave function of that state. For ^{148}Gd, in particular, the states with spin $I^\pi = 4_1^+$, 6_1^+, 8_1^+, and 10_1^+ are shown to contain one g boson, i.e., $\langle \hat{n}_g \rangle \approx 1$, and $\langle \hat{n}_g \rangle \approx 1.5$ for the 12_1^+, and 14_1^+ states.

Figures 2(c) and 2(d) depict the 0_2^+, 2_3^+, and 4_3^+ energy levels, which are supposed to be part of the excited $K^\pi = 0^+$ band in the well deformed isotopes with $N \geqslant 90$. The inclusion of g bosons has an effect of lowering the 2_3^+ and 4_3^+ energy levels for those nuclei with $N \leqslant 88$. In particular, for the 4_3^+ states of ^{148}Gd, ^{150}Gd, and ^{152}Gd the expectation values are calculated as $\langle \hat{n}_g \rangle \approx 1$. On the other hand, the hexadecapole deformation makes only a minor effect on the 0_2^+ energy levels in general, as the expectation values $\langle \hat{n}_g \rangle \approx 0$. Overall it appears that the sdg-IBM does not improve the description of these non-yrast states, and that even the *sd*-IBM, i.e., the calculation without g bosons, is able to reproduce the observed behaviors of these states rather well.

Figures 2(e) and 2(f) show the excitation spectra of the 2_2^+, 3_1^+, and 4_2^+ states, which are attributed to members of the γ vibrational band. The g boson effect appears to be minor in the description of the bandhead 2_2^+ level, but significantly lowers the energies of the 3_1^+ and 4_2^+ states for those nuclei with $N \leqslant 88$, which are weakly quadrupole and hexadecapole deformed. Particularly at $N = 84$, the 4_2^+ level obtained from the sdg-IBM is so low in energy as to be close to the 2_2^+ level, in comparison to experiment.

The discrepancies between the calculated and experimental energy spectra for non-yrast states, as observed in Figs. 2(c), 2(d), 2(e), and 2(f), are not surprising, given that, unlike the conventional IBM calculations, the Hamiltonian parameters are here not obtained from experiment, but from the mapping of the β_2-β_4 SCMF energy surface computed with the EDF that is not tailored for particular nuclei.

The detailed band structure of each nucleus can also be studied. As a representative case we show in Fig. 3 the low-energy positive-parity bands of ^{154}Gd. In the sdg-IBM spectra, states are classified into bands according to the dominant inband $E2$ transitions and according to the nature of the states in terms of the g-boson content in their wave functions. One sees from Fig. 3 that the ground-state band is reproduced well. The predicted $K^\pi = 0_2^+$ band looks stretched in energy as compared to the experimental one, even though the 0_2^+ bandhead energy is reasonably reproduced. The predicted γ band, starting from the 2_2^+ state, is much lower in energy

than the experimental one. The appearance of the low-lying 2_2^+ state indicates too pronounced γ softness, which could be attributed to the particular choice of the nuclear EDF and pairing interaction. In addition, the calculated γ band exhibits a staggering of levels, $(3_\gamma^+, 4_\gamma^+)$, $(5_\gamma^+, 6_\gamma^+)$, ... It is a characteristic of a γ-unstable rotor [51], but contradicts the observed feature of the γ band, which looks rather harmonic. To remedy this, cubic terms are often included in the boson Hamiltonian [18], since they lower the energy levels of the odd-spin members of the γ band, to be consistent with the observed γ-band structure that is harmonic. The cubic terms, however, would also lower the 2^+ bandhead energy of the γ band, which would become much lower than the experimental counterpart. Such an extension is well beyond the scope of this paper.

The theoretical band, built on top of the 4_3^+ state, is interpreted as the $K^\pi = 4^+$ band and is found to be of one-g-boson character in the present calculation. The experimental counterpart is the one with the bandhead energy $E_x(4_4^+) = 1646$ keV [49]. $E4$ transition properties are calculated with the transition operators that are given by $e_{4,\mathrm{sdg}}[\hat{Q}' + (d^\dagger \times \tilde{d})^{(4)}]$ for the sdg-IBM, and $e_{4,sd}(d^\dagger \times \tilde{d})^{(4)}$ for the sd-IBM. The addition of the $(d^\dagger \times \tilde{d})^{(4)}$ term to the $E4$ transition operator for the sdg-IBM is to compare the impact of d bosons to that of g bosons on the $E4$ transitions, and in that way one would be able to see properly how much the presence of g bosons affects the $E4$ transitions. The effective boson charges, $e_{4,\mathrm{sdg}}$ and $e_{4,sd}$, are fixed to reproduce an available experimental [49] $B(E4; 4_1^+ \to 0_1^+)$ transition rate of 38 ± 3 Weisskopf units (W.u.). The sd-IBM gives band structure of ^{154}Gd qualitatively similar to that with the sdg-IBM. The $K^\pi = 4^+$ band is also obtained in the sd-IBM with the bandhead 4_4^+ state at the excitation energy of 1412 keV. A significant difference between the sd- and sdg-IBM predictions is that the $B(E4; 4^+_{K=4^+} \to 0_1^+)$ transition obtained from the former is much lower (1.3 W.u.) than that from the latter (93 W.u.). Experiments to deduce the reduced $E4$ matrix elements, $|\langle 0_1^+ \| M(E4) \| 4_1^+ \rangle|$, were performed, e.g., in [4,5], using the (α, α') scattering and Coulomb excitations, and these transition matrix elements can be used to fix the boson effective charges, $e_{4,sd}$ and $e_{4,\mathrm{sdg}}$. However, experimental information about other $E4$ transitions is not available for the Gd isotopes under study, and hence the detailed comparison of the present model with the experimental $E4$ transition rates is not feasible. An extensive study of the $E4$ properties in other isotopic chains will be reported elsewhere.

In the deformed region, the improvement of the sdg-IBM over the sd-IBM is also visible in the higher-lying states of a given spin. For even-spin states, for example, the sixth 2^+ state and higher become lower and closer to each other in energy which is in a better agreement with experiment. For odd-spin states, this is even visible, e.g., for the third 3^+ state and higher. However, the corresponding experimental data for the 3^+ states are scarce. The sdg-IBM gives a slightly better description of the in-band $E2$ transitions, $I \to I - 2$, within ground-state band for high-spin states, e.g., $I = 8^+$ and 10^+, for deformed Gd nuclei. There is, on the other hand, no qualitative difference in the calculated $E0$, as well as $E2$, transition properties for the low-spin states between the sd-IBM and sdg-IBM. These properties will be discussed in detail in a forthcoming longer article.

IV. SUMMARY

To summarize, we have analyzed the impacts of hexadecapole deformations on the low-lying collective states of axially symmetric heavy nuclei in the spherical vibrational as well as strongly deformed regimes. By using the results of the mean-field calculations based on the relativistic EDF, the sdg-IBM Hamiltonian has been determined without any adjustment to experiment. The inclusion of g bosons has been shown to lower the states of ground-state bands with spin $I^\pi \geqslant 6^+$, especially in the region near the neutron closed shell $N = 82$, thus improving the description of vibrational nuclei. For those nuclei with large quadrupole deformation, i.e., with $N \geqslant 90$, the sdg-IBM produces the $K^\pi = 4^+$ band of one-g-boson character, which exhibits a much larger $B(E4; 4^+_{K^\pi=4^+} \to 0_1^+)$ transition than in the sd-IBM. On the other hand, the g-boson effects on low-spin non-yrast states have been shown to be marginal for most of the deformed nuclei, in which cases the sd-IBM appears to reproduce the experimental data rather well. Now that we have a way of incorporating the quadrupole and hexadecapole degrees of freedom in the IBM in a unified manner, it can be applied to identify regions of the nuclear chart, including the experimentally unexplored ones, in which hexadecapole correlations may play prominent roles.

ACKNOWLEDGMENTS

The work of L.L. is financed within the Tenure Track Pilot Programme of the Croatian Science Foundation and the École Polytechnique Fédérale de Lausanne, and the project TTP-2018-07-3554 Exotic Nuclear Structure and Dynamics, with funds from the Croatian-Swiss Research Programme.

[1] A. Bohr and B. R. Mottelson, *Nuclear Structure*, Vol. II (Benjamin, New York, USA, 1975).
[2] D. Hendrie, N. Glendenning, B. Harvey, O. Jarvis, H. Duhm, J. Saudinos, and J. Mahoney, Phys. Lett. B **26**, 127 (1968).
[3] K. A. Erb, J. E. Holden, I. Y. Lee, J. X. Saladin, and T. K. Saylor, Phys. Rev. Lett. **29**, 1010 (1972).
[4] H. Wollersheim and T. W. Elze, Nucl. Phys. A **278**, 87 (1977).
[5] R. M. Ronningen, J. H. Hamilton, L. Varnell, J. Lange, A. V. Ramayya, G. Garcia-Bermudez, W. Lourens, L. L. Riedinger, F. K. McGowan, P. H. Stelson, R. L. Robinson, and J. L. C. Ford, Phys. Rev. C **16**, 2208 (1977).
[6] C. E. Bemis, F. K. McGowan, J. L. C. Ford, W. T. Milner, P. H. Stelson, and R. L. Robinson, Phys. Rev. C **8**, 1466 (1973).

[7] N. Zamfir, G. Hering, R. Casten, and P. Paul, Phys. Lett. B **357**, 515 (1995).

[8] Y. Gupta, B. Nayak, U. Garg, K. Hagino, K. Howard, N. Sensharma, M. Şenyiğit, W. Tan, P. O'Malley, M. Smith, R. Gandhi, T. Anderson, R. deBoer, B. Frentz, A. Gyurjinyan, O. Hall, M. Hall, J. Hu, E. Lamere, Q. Liu *et al.*, Phys. Lett. B **806**, 135473 (2020).

[9] M. Spieker, S. Agbemava, D. Bazin, S. Biswas, P. Cottle, P. Farris, A. Gade, T. Ginter, S. Giraud, K. Kemper, J. Li, W. Nazarewicz, S. Noji, J. Pereira, L. Riley, M. Smith, D. Weisshaar, and R. Zegers, Phys. Lett. B **841**, 137932 (2023).

[10] W. Ryssens, G. Giacalone, B. Schenke, and C. Shen, Phys. Rev. Lett. **130**, 212302 (2023).

[11] J. Engel and J. Menéndez, Rep. Prog. Phys. **80**, 046301 (2017).

[12] F. Iachello and A. Arima, *The Interacting Boson Model* (Cambridge University Press, Cambridge, 1987).

[13] T. Otsuka, A. Arima, and F. Iachello, Nucl. Phys. A **309**, 16 (1978).

[14] T. Mizusaki and T. Otsuka, Prog. Theor. Phys. Suppl. **125**, 97 (1996).

[15] K. Nomura, N. Shimizu, and T. Otsuka, Phys. Rev. Lett. **101**, 142501 (2008).

[16] K. Nomura, N. Shimizu, and T. Otsuka, Phys. Rev. C **81**, 044307 (2010).

[17] K. Nomura, T. Otsuka, N. Shimizu, and L. Guo, Phys. Rev. C **83**, 041302(R) (2011).

[18] K. Nomura, N. Shimizu, D. Vretenar, T. Nikšić, and T. Otsuka, Phys. Rev. Lett. **108**, 132501 (2012).

[19] K. Nomura, D. Vretenar, and B.-N. Lu, Phys. Rev. C **88**, 021303(R) (2013).

[20] K. Nomura, D. Vretenar, T. Nikšić, and B.-N. Lu, Phys. Rev. C **89**, 024312 (2014).

[21] A. Bohr and B. R. Mottelson, Phys. Scr. **22**, 468 (1980).

[22] T. Otsuka, Nucl. Phys. A **368**, 244 (1981).

[23] T. Otsuka, A. Arima, and N. Yoshinaga, Phys. Rev. Lett. **48**, 387 (1982).

[24] D. R. Bes, R. A. Broglia, E. Maglione, and A. Vitturi, Phys. Rev. Lett. **48**, 1001 (1982).

[25] P. Van Isacker, K. Heyde, M. Waroquier, and G. Wenes, Nucl. Phys. A **380**, 383 (1982).

[26] T. Otsuka and J. N. Ginocchio, Phys. Rev. Lett. **55**, 276 (1985).

[27] T. Otsuka and M. Sugita, Phys. Lett. B **215**, 205 (1988).

[28] Y. D. Devi and V. K. B. Kota, Z. Phys. A **337**, 15 (1990).

[29] S. Kuyucak, Nucl. Phys. A **570**, 187 (1994).

[30] S. Zerguine, P. Van Isacker, A. Bouldjedri, and S. Heinze, Phys. Rev. Lett. **101**, 022502 (2008).

[31] P. Van Isacker, A. Bouldjedri, and S. Zerguine, Nucl. Phys. A **836**, 225 (2010).

[32] P. Cejnar, J. Jolie, and R. F. Casten, Rev. Mod. Phys. **82**, 2155 (2010).

[33] P. Ring and P. Schuck, *The Nuclear Many-Body Problem* (Springer-Verlag, Berlin, 1980).

[34] M. Bender, P.-H. Heenen, and P.-G. Reinhard, Rev. Mod. Phys. **75**, 121 (2003).

[35] L. M. Robledo, T. R. Rodríguez, and R. R. Rodríguez-Guzmán, J. Phys. G: Nucl. Part. Phys. **46**, 013001 (2019).

[36] D. Vretenar, A. V. Afanasjev, G. A. Lalazissis, and P. Ring, Phys. Rep. **409**, 101 (2005).

[37] J. Meng, H. Toki, S. Zhou, S. Zhang, W. Long, and L. Geng, Prog. Part. Nucl. Phys. **57**, 470 (2006).

[38] T. Nikšić, D. Vretenar, and P. Ring, Prog. Part. Nucl. Phys. **66**, 519 (2011).

[39] J. Meng and S. G. Zhou, J. Phys. G: Nucl. Part. Phys. **42**, 093101 (2015).

[40] S.-G. Zhou, Phys. Scr. **91**, 063008 (2016).

[41] G. Lalazissis, S. Raman, and P. Ring, At. Data Nucl. Data Tables **71**, 1 (1999).

[42] C. V. N. Kumar and L. M. Robledo, Phys. Rev. C **108**, 034312 (2023).

[43] B.-N. Lu, J. Zhao, E.-G. Zhao, and S.-G. Zhou, Phys. Rev. C **89**, 014323 (2014).

[44] T. Nikšić, D. Vretenar, and P. Ring, Phys. Rev. C **78**, 034318 (2008).

[45] Y. Tian, Z. Y. Ma, and P. Ring, Phys. Lett. B **676**, 44 (2009).

[46] W. Nazarewicz and P. Rozmej, Nucl. Phys. A **369**, 396 (1981).

[47] V. K. B. Kota, J. Van der Jeugt, H. De Meyer, and G. Vanden Berghe, J. Math. Phys. **28**, 1644 (1987).

[48] J. N. Ginocchio and M. W. Kirson, Nucl. Phys. A **350**, 31 (1980).

[49] Brookhaven National Nuclear Data Center, http://www.nndc.bnl.gov.

[50] S. Heinze, computer program ARBMODEL, University of Cologne, 2008.

[51] L. Wilets and M. Jean, Phys. Rev. **102**, 788 (1956).